A Theoretical Study of the ^{2}NCO + ^{2}OH Reaction

Pablo Campomanes, Isabel Menéndez, and Tomás L. Sordo*

Departamento de Química Física y Analítica, Facultad de Química, Universidad de Oviedo, C/Julián Clavería, 8, 33006 Oviedo, Principado de Asturias, Spain

Received: July 31, 2000; In Final Form: October 18, 2000

Four reaction channels for the title reaction were theoretically studied at the B3LYP/6-311++G(d,p) theory level. At 298.15 K the most favorable route to HCO + NO (reaction 1) is the singlet one with an energy barrier of 15.3 kcal/mol in close agreement with the reported value of 15.0 kcal/mol. Both the singlet and the triplet pathways to yield CO + NO + H (reaction 2) are kinetically competitive with an energy barrier of 20.7 kcal/mol. The triplet channels to HNCO + O (reaction 3) and to NCOH + O (reaction 4) present an energy barrier at 298.15 K of 11.5 and 29.6 kcal/mol, respectively, whereas those for the corresponding reverse processes are 16.2 and 5.9 kcal/mol to compare with the reported values of 11.4 and 4.0 kcal/mol, respectively. Except for reaction 2 the rate determining TSs remain the same at higher temperatures. The triplet pathway to HNCO + O is the most favored one at the three temperatures considered in this work: 298.15, 1000, and 1500 K. At higher temperatures reaction 4 remains the most disfavored kinetically but the Gibbs energy barriers for reactions 1−3 become closer the higher the temperature so that at 1500 K reactions 1 and 2 are competitive with reaction 3. These trends would agree with the increase of the concentration of NO and the decrease of the concentration of HNCO found experimentally. It is interesting to note that reaction 2, which has been found to be a high rate and sensitive reaction by reaction-path analysis, is the most kinetically favored one by an increase of temperature.

Introduction

Interest in the combustion chemistry of nitrogen compounds derives from the role of nitrogen oxides, collectively known as NO_x, in our environment. Increasingly sophisticated approaches for the control of NO_x formation during combustion are required nowadays.

NCO is a relatively stable radical that can react with other radical to break the N−C bond. Hydrogen abstraction from most species is also a very probable process.[1] The reaction of NCO with OH via the four following reaction channels:

$$^2\text{NCO} + {}^2\text{OH} \rightarrow {}^2\text{HCO} + {}^2\text{NO} \quad (1)$$

$$\rightarrow {}^1\text{CO} + {}^2\text{NO} + {}^2\text{H} \quad (2)$$

$$\rightarrow {}^1\text{HNCO} + {}^3\text{O} \quad (3)$$

$$\rightarrow {}^1\text{NCOH} + {}^3\text{O} \quad (4)$$

has been proposed to participate in several important processes in the combustion chemistry of nitrogen. The first process has been identified as a step for homogeneous NO formation and reduction.[2,3] The second one has been included in the set of reactions that are known to be important in prompt NO formation and fuel-nitrogen conversion.[2] The third channel has been proposed by Klaus and Warnatz as taking part in the mechanism for the formation and reduction of NO_x.[4,5] The four channels appear in the mechanism for methylamine oxidation in flow reactors.[6]

As a considerable insight into the four above-mentioned reaction mechanisms can be gained from theoretical electronic structure calculations, in the present work we address a density functional theory (DFT) study of these processes at several temperatures, trying to get information useful for the analysis of the important combustion processes mentioned above.

Methods

Full optimizations by means of Schlegel's algorithm[7] at the B3LYP DFT level[8] with the 6-311++G(d,p) basis set were performed using the Gaussian 98 program.[9] The nature of the stationary points was further checked and zero point vibrational energies (ZPVEs) were evaluated by analytical computations of harmonic vibrational frequencies at the same theory level. Intrinsic reaction coordinate (IRC) calculations at the same level were also carried out to check the connection between all the critical structures located using the Gonzalez and Schlegel method[10] implemented in Gaussian 98.

ΔH, ΔS and ΔG values were also calculated to obtain results more readily comparable with experiment within the ideal gas, rigid rotor, and harmonic oscillator approximations.[11] A pressure of 1 atm and temperatures of 298.15, 1000, and 1500 K were assumed in the calculations.

Results and Discussion

We will present first the results obtained for the B3LYP/6-311++G(d,p) electronic potential energy surface (PES) corresponding to reactions 1−4 and then we will discuss the effect of thermal corrections and entropy on these processes. For reactions 1 and 2 two different spin couplings are possible and therefore we investigated both the corresponding singlet and triplet PESs. For reactions 3 and 4 we investigated the triplet PES. The subscripts in the names of the critical structures indicate the reactions in which they appear.

* To whom correspondence should be addressed. E-mail: tsordo@correo.uniovi.es. Fax: +34 98 510 31 25.

10.1021/jp002732j CCC: $20.00
Published on Web 12/09/2000

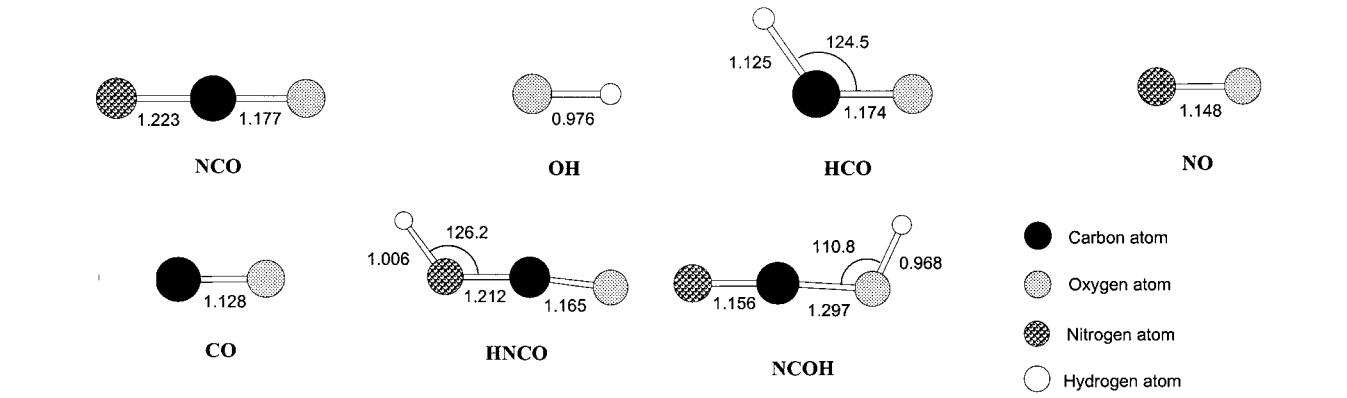

Figure 1. Optimized geometries of the reactants and products for the title reaction. Bond lengths are given in Å and angles in degrees.

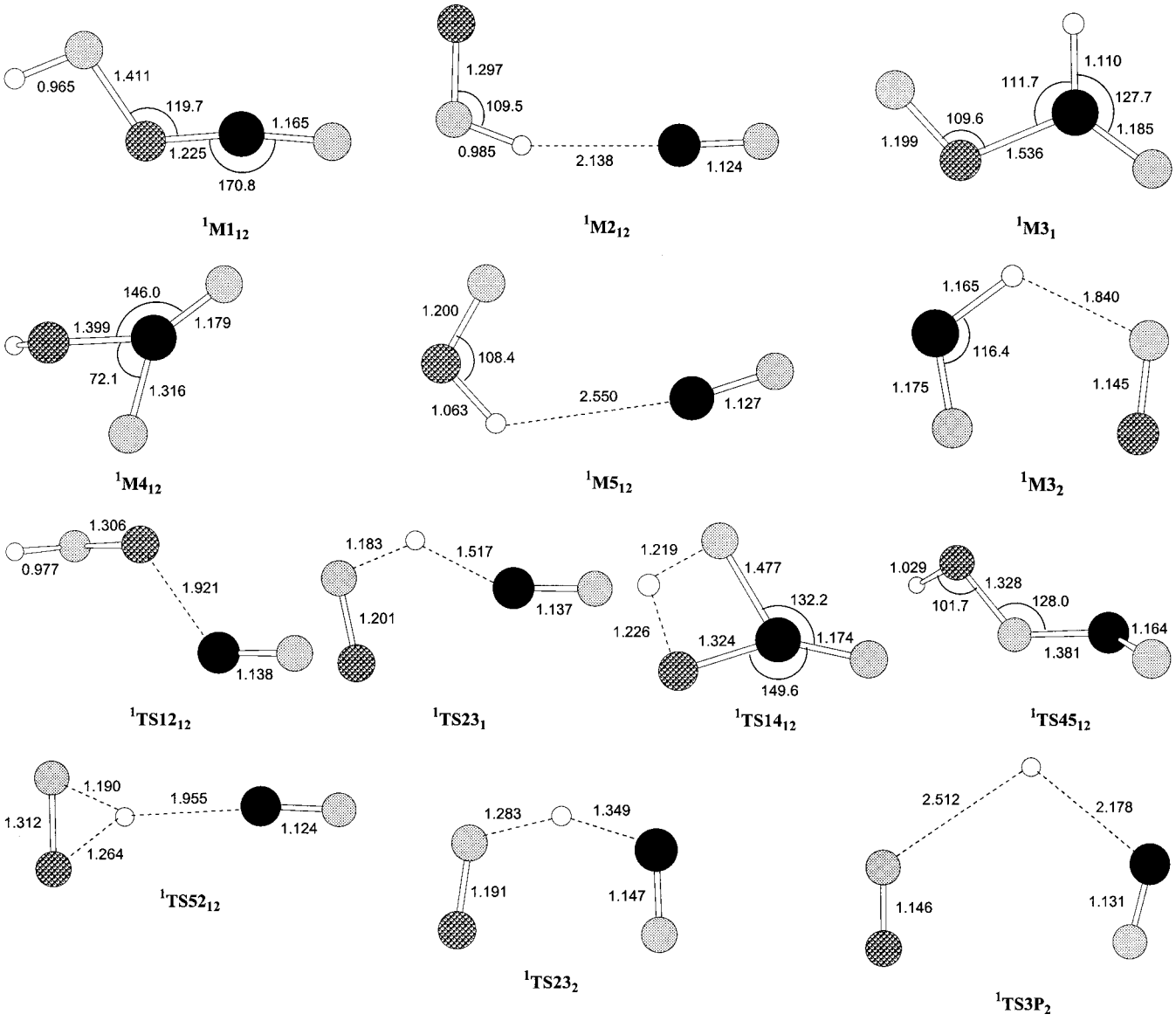

Figure 2. Optimized geometries of the minima and TSs located in this work along the singlet channels for the title reaction. Bond lengths are given in Å and angles in degrees.

Figure 1 presents the geometry of the reactants and products for reactions 1−4, and Figures 2 and 3 display, respectively, the geometry of the singlet and triplet critical structures located along the reaction coordinates. Figures 4 and 5 show the electronic energy profiles (including the ZPVE) corresponding to the singlet and triplet pathways, respectively, for the four reactions. Unless otherwise stated, the electronic energy including the ZPVE will be given in the text.

Reaction ^{2}NCO + ^{2}OH → ^{2}HCO + ^{2}NO. Tables 1 and 2 display the energy corresponding to the singlet and triplet critical structures located for this reaction.

Singlet PES. The channel on the singlet PES may proceed

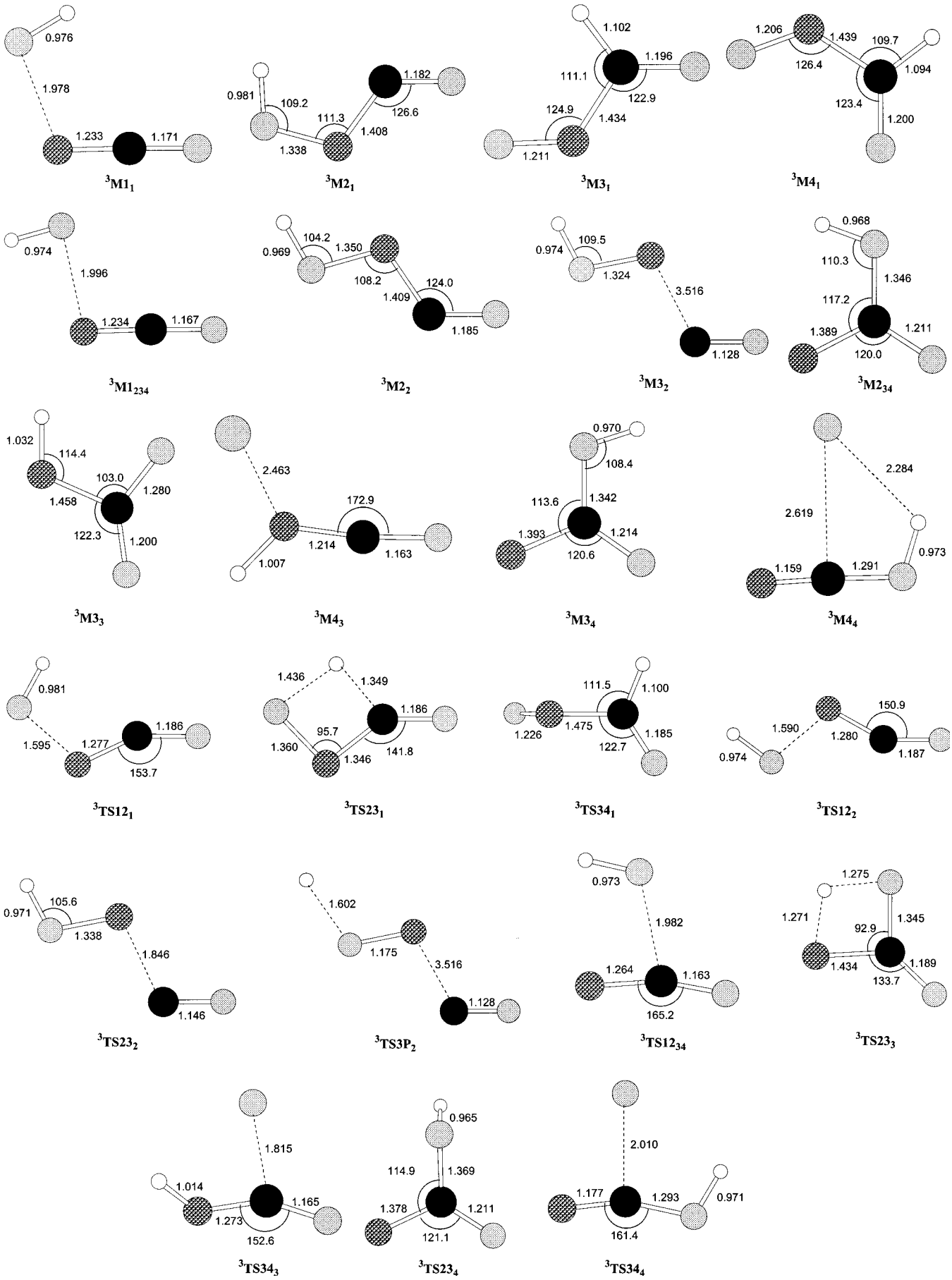

Figure 3. Optimized geometries of the minima and TSs located in this work along the triplet channels for the title reaction. Bond lengths are given in Å and angles in degrees.

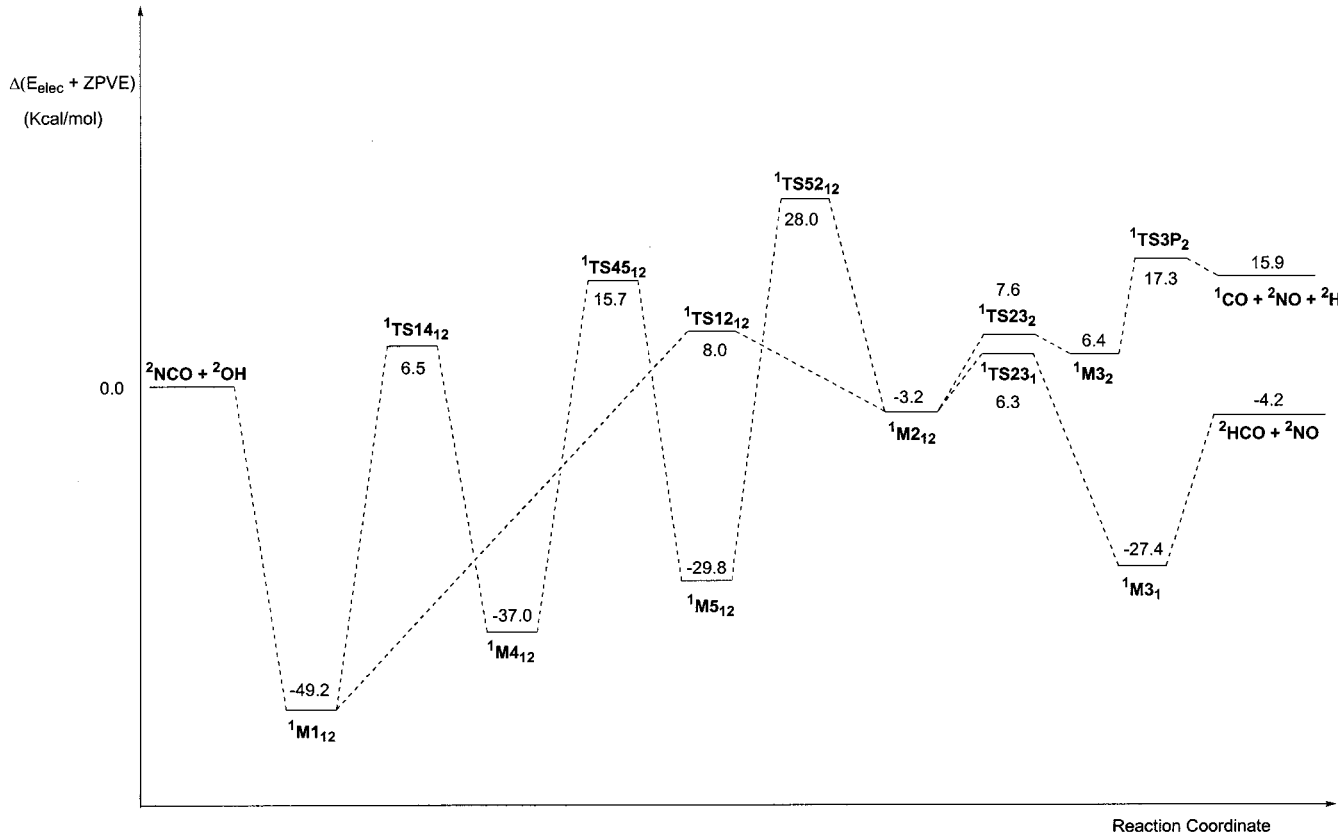

Figure 4. Electronic energy profiles including ZPVE corresponding to the singlet reaction channels for the title reaction.

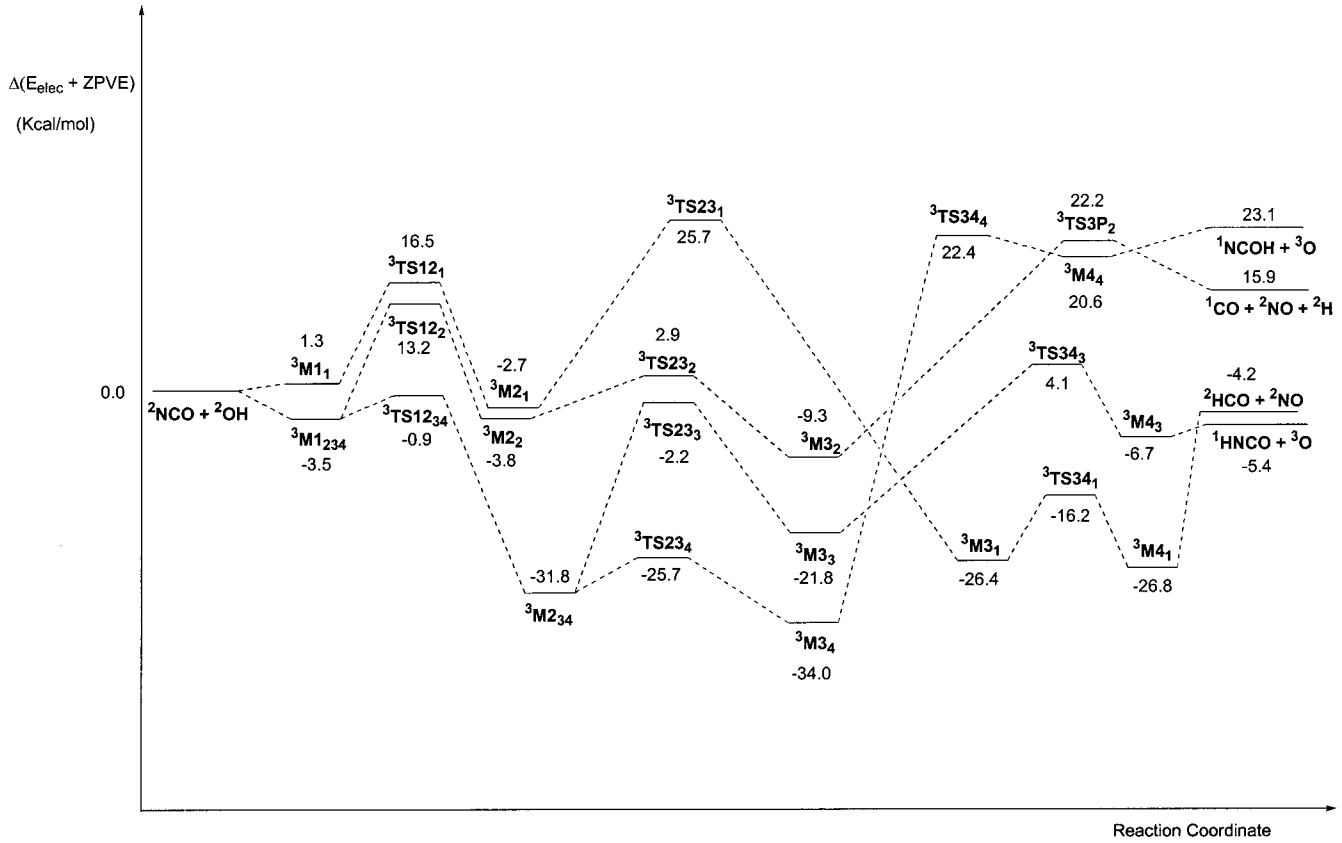

Figure 5. Electronic energy profiles including ZPVE corresponding to the triplet reaction channels for the title reaction.

through two different pathways starting at the intermediate $^1M1_{12}$, which is 49.2 kcal/mol more stable than the reactants, and forms by recombination of NCO and OH with formation of a N−O bond. From $^1M1_{12}$ the first pathway proceeds through TS $^1TS12_{12}$, 8.0 kcal/mol above the reactants, for the breaking of the N−C bond to give the complex $^1M2_{12}$, which is 3.2 kcal/

TABLE 1: Relative Electronic Energies, Zero-Point Vibrational Energy Corrections (ZPVE), and Free Energies for the Structures Located along the Singlet Pathways for Reactions 1 and 2[a]

species	ΔE_{elec}	ZPVE	$\Delta(E_{elec}$ + ZPVE)	ΔG 298.15 K	ΔG 1000 K	ΔG 1500 K
			Reactions 1 and 2			
^{2}NCO + ^{2}OH	0.0	11.6	0.0	0.0	0.0	0.0
^{1}M1$_{12}$	−54.0	16.4	−49.2	−41.1	−18.9	−3.2
^{1}M2$_{12}$	−4.6	13.0	−3.2	2.3	14.7	23.0
^{1}M4$_{12}$	−42.0	16.6	−37.0	−28.5	−3.7	13.8
^{1}M5$_{12}$	−31.2	12.9	−29.8	−24.5	−12.6	−4.6
^{1}TS12$_{12}$	6.3	13.2	8.0	15.3	35.1	49.4
^{1}TS14$_{12}$	5.4	12.7	6.5	14.9	39.3	56.9
^{1}TS45$_{12}$	13.2	14.1	15.7	23.7	46.5	63.0
^{1}TS52$_{12}$	29.7	9.8	28.0	34.0	48.4	67.0
			Reaction 1			
^{1}M3$_1$	−31.0	15.2	−27.4	−19.5	2.4	17.9
^{1}TS23$_1$	6.5	11.3	6.3	13.5	33.6	47.9
^{2}HCO + ^{2}NO	−3.6	11.0	−4.2	−5.9	−9.3	−11.2
			Reaction 2			
^{1}M3$_2$	4.4	13.6	6.4	14.3	35.5	50.3
^{1}TS23$_2$	8.5	10.7	7.6	15.2	36.4	50.1
^{1}TS3P$_2$	22.1	6.8	17.3	20.7	25.8	28.9
^{1}CO + ^{2}NO + ^{2}H	21.5	6.0	15.9	9.1	−10.5	−24.7

[a] The values are given in kcal/mol.

TABLE 2: Relative Electronic Energies, Zero-Point Vibrational Energy Corrections (ZPVE), and Free Energies for the Structures Located along the Triplet Pathway for Reaction 1[a]

species	ΔE_{elec}	ZPVE	$\Delta(E_{elec}$ + ZPVE)	ΔG 298.15 K	ΔG 1000 K	ΔG 1500 K
^{2}NCO + ^{2}OH	0.0	11.6	0.0	0.0	0.0	0.0
^{3}M1$_1$	−0.9	13.8	1.3	8.0	25.0	36.6
^{3}TS12$_1$	14.5	13.6	16.5	24.0	45.5	61.1
^{3}M2$_1$	−6.3	15.2	−2.7	4.9	26.1	41.0
^{3}TS23$_1$	25.4	11.9	25.7	33.4	56.2	72.5
^{3}M3$_1$	−30.2	15.4	−26.4	−18.8	2.8	18.1
^{3}TS34$_1$	−19.5	14.9	−16.2	−8.6	14.5	31.5
^{3}M4$_1$	−31.0	15.8	−26.8	−19.3	2.6	18.1
^{2}HCO + ^{2}NO	−3.6	11.0	−4.2	−5.9	−9.3	−11.2

[a] The values are given in kcal/mol.

mol more stable than the separate reactants. In ^{1}M2$_{12}$ CO and NOH are interacting through C and H atoms separated by a distance of 2.138 Å. ^{1}M2$_{12}$ is connected with the intermediate ^{1}M3$_1$ through TS ^{1}TS23$_1$, which is 6.3 kcal/mol above the reactants. ^{1}M3$_1$ is a molecule of nitrosoformaldehyde, 27.4 kcal/mol more stable than the reactants, in which the two oxygen atoms are in a trans orientation. Finally, ^{1}M3$_1$ dissociates into the products HCO + NO, 4.2 kcal/mol under the original reactants. The second pathway proceeds from ^{1}M1$_{12}$ to the intermediate ^{1}M4$_{12}$ through TS ^{1}TS14$_{12}$, 6.5 kcal/mol above the reactants, for the addition of OH across the N−C bond. ^{1}M4$_{12}$ is 12.2 kcal/mol less stable than ^{1}M1$_{12}$ and is connected with the complex ^{1}M5$_{12}$, in which HNO is interacting with CO with a distance H···C of 2.550 Å, through TS ^{1}TS45$_{12}$ for the insertion of the oxygen atom into the N−C bond. ^{1}M5$_{12}$ is 7.2 kcal/mol above ^{1}M4$_{12}$ and ^{1}TS45$_{12}$ is 15.7 kcal/mol less stable than the reactants. Finally, ^{1}M5$_{12}$ proceeds into ^{1}M2$_{12}$ through TS ^{1}TS52$_{12}$, 28.0 kcal/mol above the reactants, for the isomerization of the HNO moiety in ^{1}M5$_{12}$ to the NOH moiety in ^{1}M2$_{12}$ assisted by the CO fragment whose C atom is interacting with the shifting H atom.

Triplet PES. The first critical structure located on the triplet PES is a pre-reactive complex ^{3}M1$_1$, in which the OH interacts with the nitrogen atom of NCO with the H atom oriented inward. ^{3}M1$_1$ is 0.9 kcal/mol more stable than the separate reactants in electronic energy and becomes a transient structure when the ZPVE correction is included. The next structure located along the reaction coordinate is a TS 16.5 kcal/mol above the reactants, ^{3}TS12$_1$, for the O addition of OH to the N atom of NCO trans relative to the N−C bond; this addition produces bending of NCO to give the minimum structure ^{3}M2$_1$, 2.7 kcal/mol more stable than the reactants. ^{3}M2$_1$ evolves through ^{3}TS23$_1$ for the 1,3 transposition of the H atom to yield the minimum ^{3}M3$_1$, with an energy barrier of 28.4 kcal/mol. ^{3}M3$_1$ yields the intermediate ^{3}M4$_1$, 0.4 kcal/mol more stable than it, through TS ^{3}TS34$_1$ for the rotation of the N−O moiety about the N−C bond to locate the two oxygen atoms in a cis orientation with an energy barrier of 10.2 kcal/mol. Finally, ^{3}M4$_1$ undertakes a barrierless dissociation into HCO and NO, which are 4.2 kcal/mol under the reactants.

Reaction ^{2}NCO + ^{2}OH → ^{1}CO + ^{2}NO + ^{2}H. Tables 1 and 2 display the energy corresponding to singlet and triplet critical structures, respectively, located for this reaction.

Singlet PES. The singlet pathway for this channel has in common with the singlet channel of reaction 1 the structures from the reactants to ^{1}M2$_{12}$. From ^{1}M2$_{12}$ the system evolves now through ^{1}TS23$_2$ for the transfer of H from the O atom to the C atom to give ^{1}M3$_2$. ^{1}TS23$_2$ and ^{1}M3$_2$ are 7.6 and 6.4 kcal/mol above the reactants, respectively. Finally, the complex ^{1}M3$_2$ dissociates into the products CO + NO + H, 15.9 kcal/mol above the reactants, through TS ^{1}TS3P$_2$, which presents an energy barrier of 10.9 kcal/mol with respect to ^{1}M3$_2$.

Triplet PES. The first critical structure located along this triplet channel is a pre-reactive complex, ^{3}M1$_{234}$, 3.5 kcal/mol more stable than the reactants, in which the oxygen atom of OH interacts with the N atom of NCO at a distance of 1.996 Å, with the H atom oriented outward. ^{3}M1$_{234}$ proceeds through TS ^{3}TS12$_2$ for the addition of OH to NCO with an energy barrier

TABLE 3: Relative Electronic Energies, Zero-Point Vibrational Energy Corrections (ZPVE), and Free Energies for the Structures Located along the Triplet Pathway for Reaction 2[a]

				ΔG		
species	ΔE_{elec}	ZPVE	$\Delta(E_{elec}+\text{ZPVE})$	298.15 K	1000 K	1500 K
$^2NCO + {}^2OH$	0.0	11.6	0.0	0.0	0.0	0.0
$^3M1_{234}$	−6.1	14.1	−3.5	3.3	21.3	33.6
$^3TS12_2$	10.9	13.9	13.2	20.7	42.4	58.1
$^3M2_2$	−7.8	15.5	−3.8	3.7	24.8	39.5
$^3TS23_2$	1.0	13.5	2.9	9.9	29.0	42.9
$^3M3_2$	−9.5	11.7	−9.3	−10.9	−14.2	−16.1
$^3TS3P_2$	27.3	6.5	22.2	20.4	16.3	13.9
$^1CO + {}^2NO + {}^2H$	21.5	6.0	15.9	9.1	−10.5	−24.7

[a] The values are given in kcal/mol.

TABLE 4: Relative Electronic Energies, Zero-Point Vibrational Energy Corrections (ZPVE), and Free Energies for the Structures Located along the Triplet Pathways for Reactions 3 and 4[a]

				ΔG		
species	ΔE_{elec}	ZPVE	$\Delta(E_{elec}+\text{ZPVE})$	298.15 K	1000 K	1500 K
			Reactions 3 and 4			
$^2NCO + {}^2OH$	0.0	11.6	0.0	0.0	0.0	0.0
$^3M1_{234}$	−6.1	14.1	−3.5	3.3	21.3	33.6
$^3TS12_{34}$	−2.7	13.4	−0.9	6.4	26.7	41.3
$^3M2_{34}$	−35.8	15.6	−31.8	−24.2	−2.5	12.7
			Reaction 3			
$^3TS23_3$	−3.3	12.6	−2.2	5.5	28.8	45.6
$^3M3_3$	−24.4	14.2	−21.8	−14.3	6.4	20.7
$^3TS34_3$	1.8	13.8	4.1	11.5	32.8	48.2
$^3M4_3$	−8.9	13.8	−6.7	−1.2	12.7	22.0
$^1HNCO + {}^3O$	−7.2	13.3	−5.4	−4.7	−2.4	−0.9
			Reaction 4			
$^3TS23_4$	−25.7	14.6	−25.7	−18.0	4.9	21.5
$^3M3_4$	−34.0	15.8	−34.0	−26.4	−4.4	11.0
$^3TS34_4$	22.4	13.9	22.4	29.6	56.8	75.7
$^3M4_4$	20.6	14.0	20.6	26.2	55.4	74.0
$^1NCOH + {}^3O$	23.1	13.5	23.1	23.7	30.4	34.7

[a] The values are given in kcal/mol.

with respect to $^3M1_{234}$ of 16.7 kcal/mol, to give the intermediate $^3M2_2$, which is 3.8 kcal/mol more stable than the reactants. $^3M2_2$ dissociates into the radicals NOH and CO, $^3M3_2$, 9.3 kcal/mol under the reactants through TS $^3TS23_2$, which is 2.9 kcal/mol less stable than the reactants. NOH in turn dissociates into H and NO to give the final products 15.9 kcal/mol above the separate reactants through TS $^3TS3P_2$, which is 22.2 kcal/mol less stable than the reactants.

Reaction $^2NCO + {}^2OH \rightarrow {}^1HNCO + {}^3O$. Table 3 displays the energy corresponding to the critical structures located for this reaction.

This triplet channel starts at the pre-reactive complex $^3M1_{234}$, like the triplet pathway of channel (2) presented above, but now $^3M1_{234}$ evolves through $^3TS12_{34}$, which is 2.6 kcal/mol above it, to give the intermediate $^3M2_{34}$, 31.8 kcal/mol more stable than the reactants. In $^3M2_{34}$ the oxygen atom of the hydroxyl moiety is bonded to the carbon atom and the hydrogen atom is in a cis relationship with the nitrogen atom. $^3M2_{34}$ evolves through TS $^3TS23_3$, 29.6 kcal/mol above it, for the H transfer from the O atom to the N atom to give the intermediate $^3M3_3$. $^3M3_3$ is 21.8 kcal/mol under the separate reactants and evolves through TS $^3TS34_3$, 4.1 kcal/mol above the reactants, to give the pre-product complex $^3M4_3$, 6.7 kcal/mol more stable than the reactants. In $^3M4_3$ the oxygen atom originally forming the OH radical is weakly linked to the nitrogen atom at a distance of 2.463 Å. Finally, $^3M4_3$ dissociates into the products HNCO + O without encountering any energy barrier. This channel is exoergic by 5.4 kcal/mol.

Reaction $^2NCO + {}^2OH \rightarrow {}^1NCOH + {}^3O$. Table 4 displays the energy corresponding to the critical structures located for this reaction.

This triplet channel has in common with the previous one the structures $^3M1_{234}$, $^3TS12_{34}$ and $^3M2_{34}$. $^3M2_{34}$ may evolve through TS $^3TS23_4$, 6.1 kcal/mol above it, for the rotation of the OH moiety about the C−O bond to give the intermediate $^3M3_4$, 34.0 kcal/mol under the reactants. In $^3M3_4$ the hydrogen atom is in a trans relationship with the nitrogen atom. $^3M3_4$ evolves through TS $^3TS34_4$, 22.4 kcal/mol above the reactants, for the migration of the hydrogen atom from one oxygen atom to the other while the former oxygen atom separates from the rest of the system to yield the pre-product complex $^3M4_4$, 20.6 kcal/mol above the reactants, in which the oxygen atom is situated at a distance of 2.619 Å from the carbon atom. Finally, $^3M4_4$ dissociates without encountering any energy barrier into the products NCOH + O, which are 23.1 kcal/mol above the reactants.

Gibbs Energy Profiles and Kinetic Constants. Figures 6 and 7 display the Gibbs energy profiles for the singlet pathways (reactions 1 and 2) at 298.15 and 1500 K, respectively, and Figures 8 and 9 those for the four triplet pathways at the same temperatures. Tables 1−4 collect the ΔG values for all the structures involved in reactions 1−4 at 298.15, 1000, and 1500 K.

When thermal corrections and entropy are taken into account at 298.15 K, the singlet energy profiles (see Figure 6) become destabilized with respect to the reactants by about 3−12 kcal/mol except for the products of both channels. The products CO + NO + H are indeed quite favored by the entropic component. According to our calculations, the most favorable pathway to HCO + NO is the singlet one with an energy barrier of 15.3 kcal/mol ($^1TS12_{12}$), in excellent agreement with the reported value of 15.0 kcal/mol.[6] The barrier corresponding to $^1TS12_{12}$

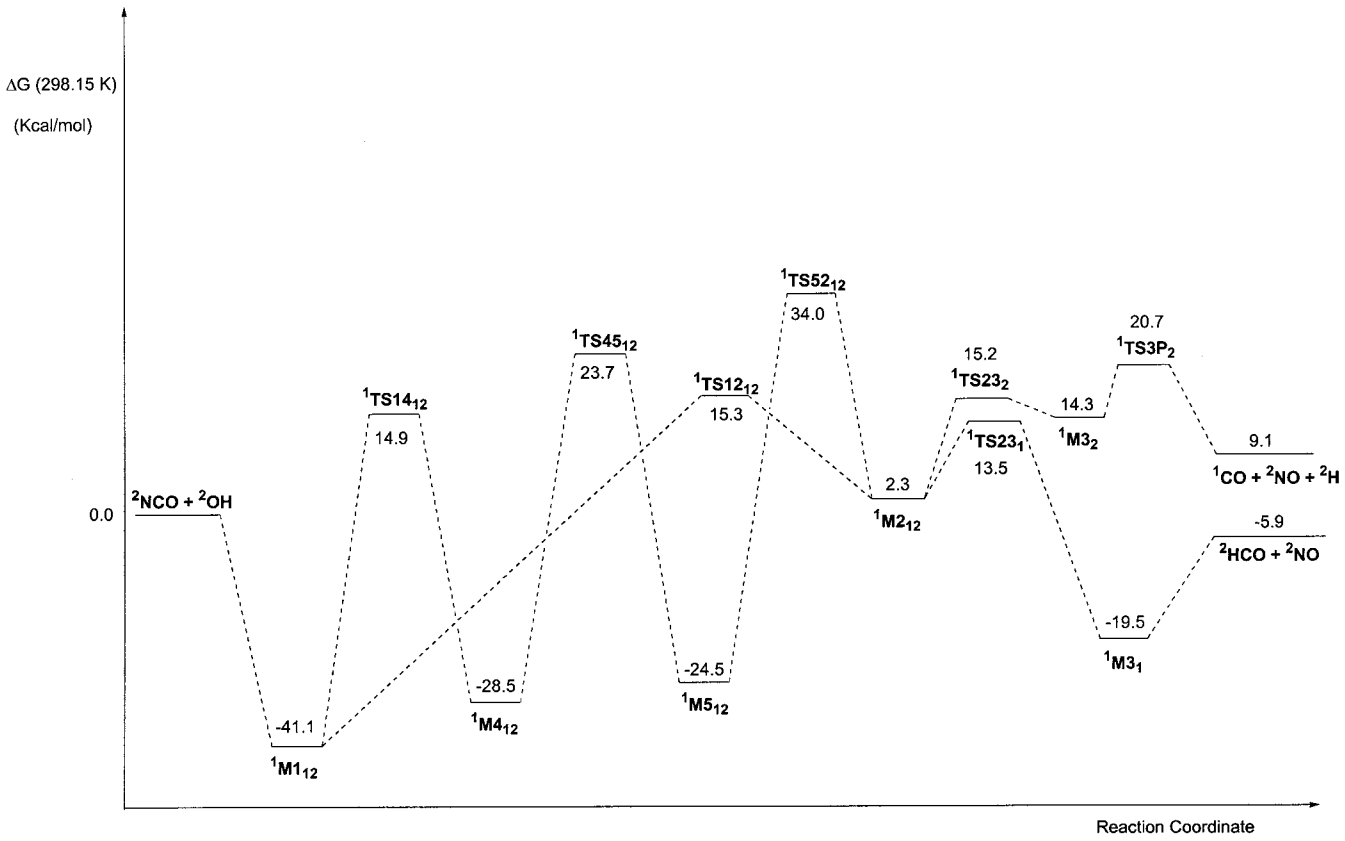

Figure 6. Free energy profiles at 298.15 K corresponding to the singlet reaction channels for the title reaction.

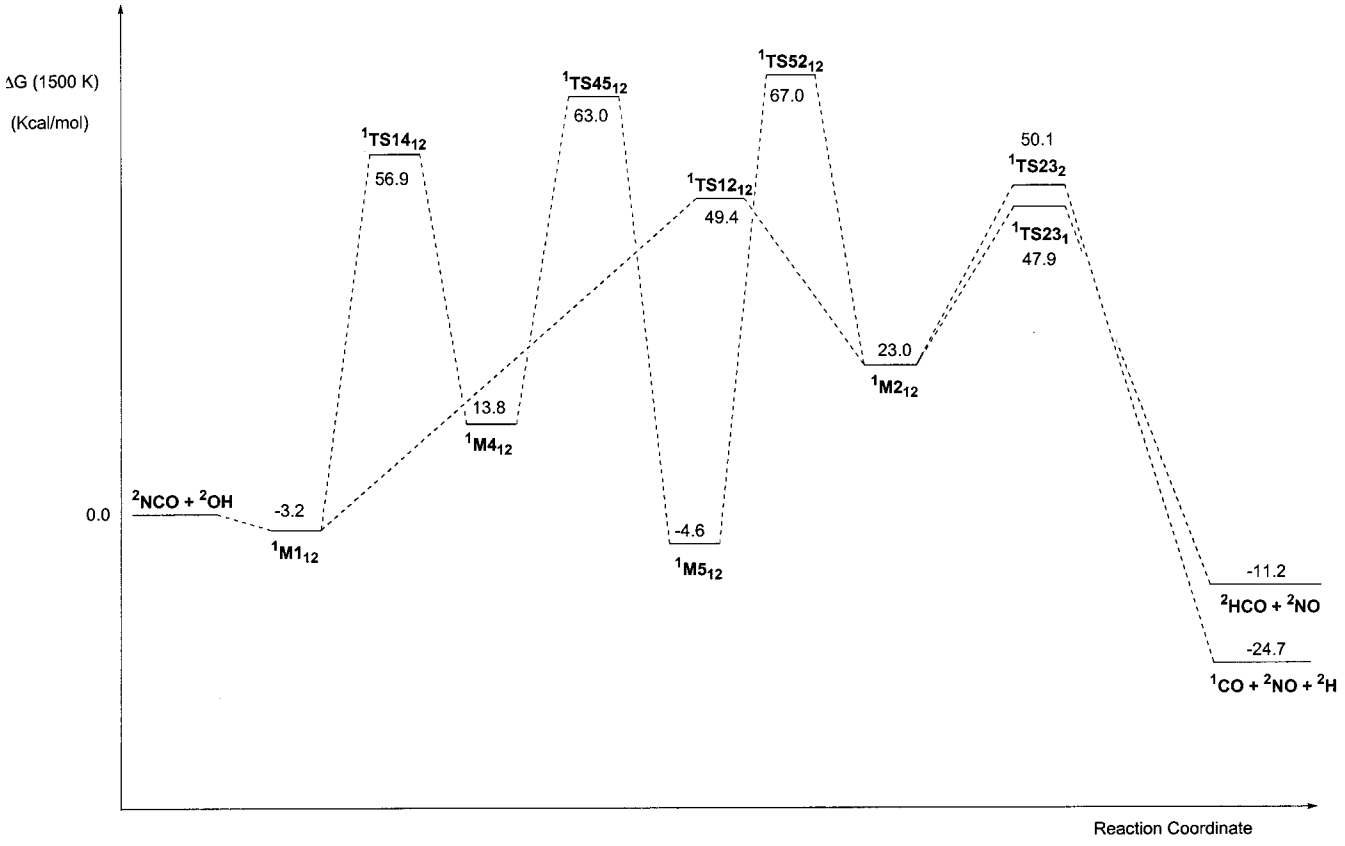

Figure 7. Free energy profiles at 1500 K corresponding to the singlet reaction channels for the title reaction.

originates mainly from the partial rupture of the C═N bond in ^{1}M1$_{12}$. The energy barrier for the singlet pathway to CO + NO + H is 20.7 kcal/mol (^{1}TS3P$_2$) to compare with the value of 16.3 kcal/mol estimated by transition state theory (TST).[6] Although ^{1}TS3P$_2$ is favored by entropy, a barrier results from the rupture of a C−H bond in ^{1}M3$_2$.

The triplet free energy profiles at 298.15 K (see Figure 8) become also destabilized with respect to the electronic energy

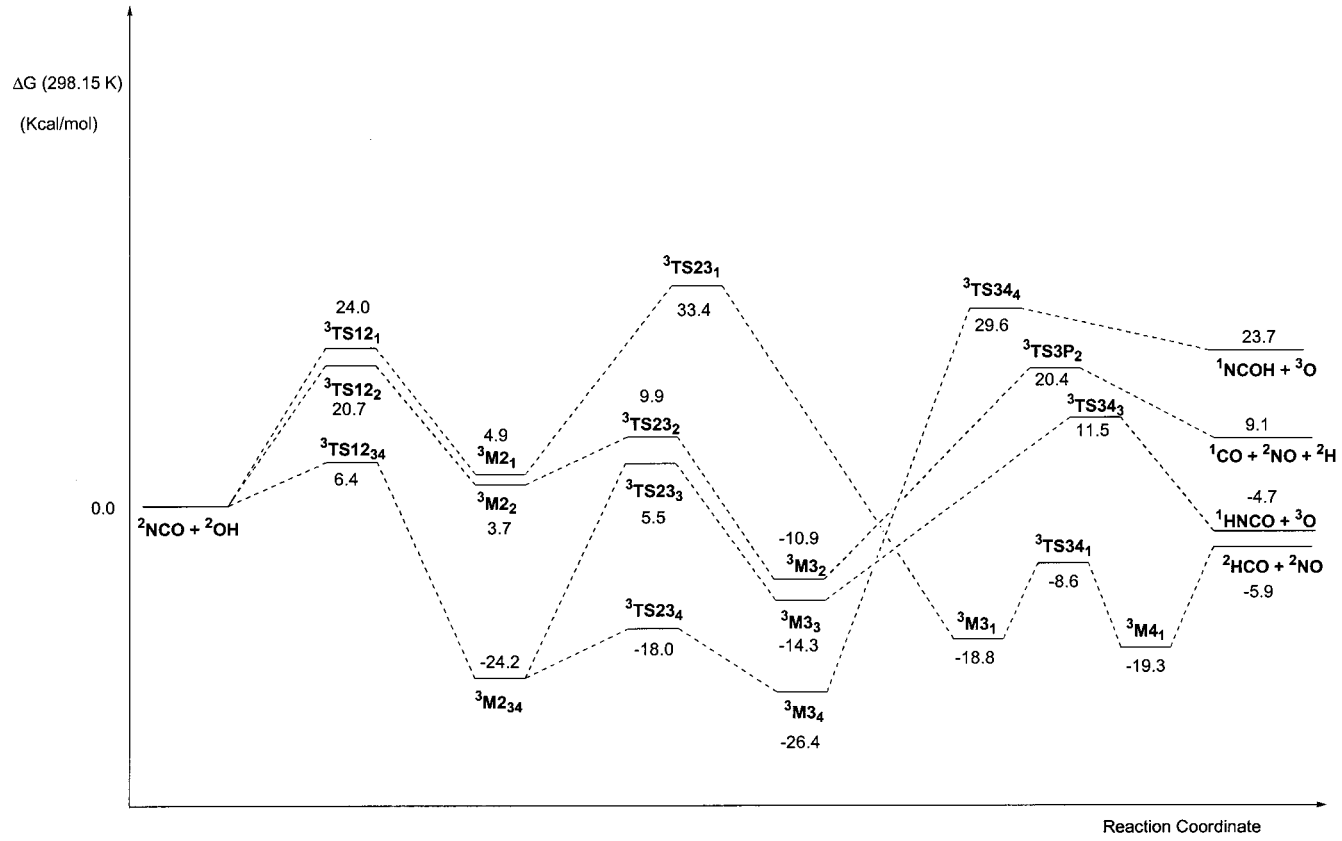

Figure 8. Free energy profiles at 298.15 K corresponding to the triplet reaction channels for the title reaction.

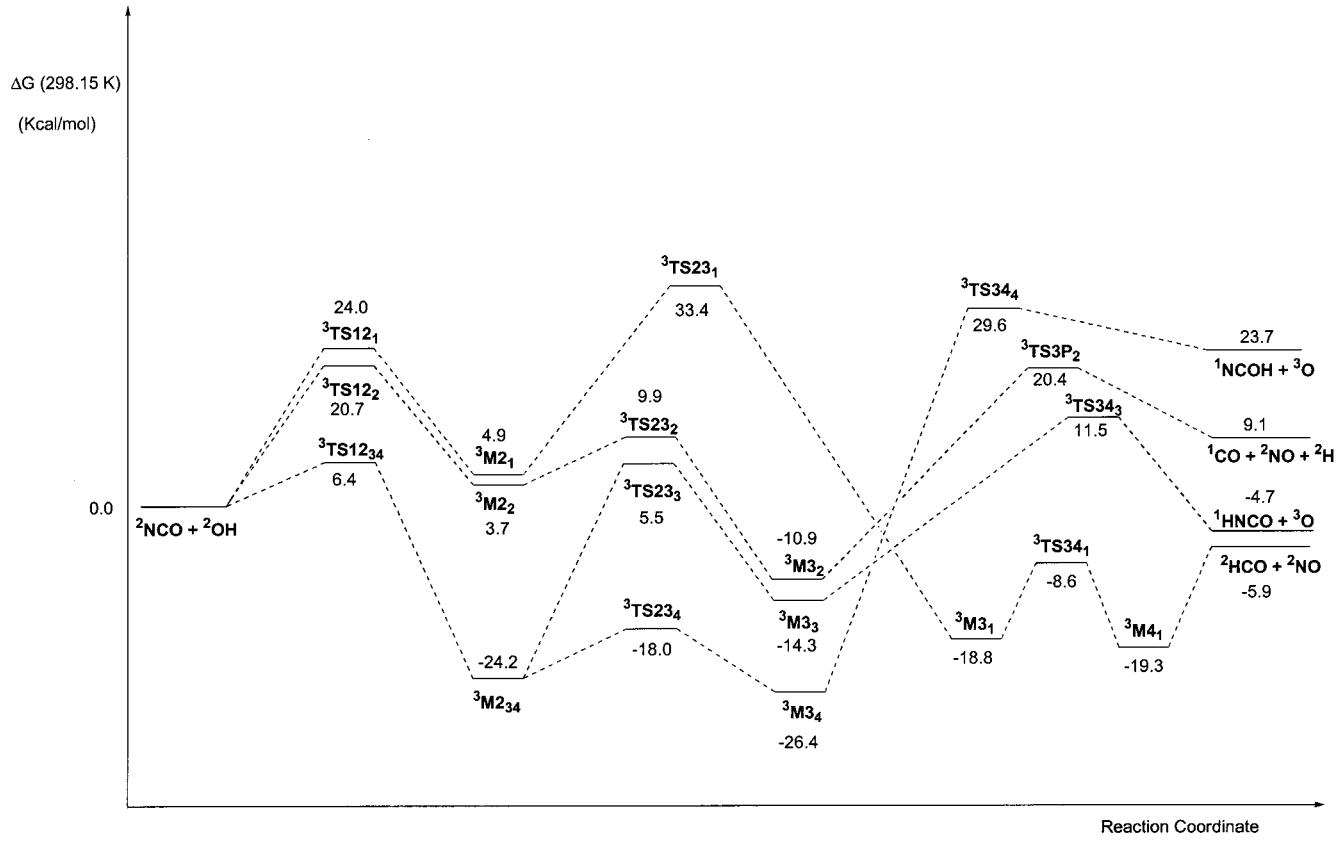

Figure 9. Free energy profiles at 1500 K corresponding to the triplet reaction channels for the title reaction.

ones including the ZPVE by about 1−9 kcal/mol, except for $^3M3_2$, $^3TS3P_2$ and the products for channels (1) and (2). As a consequence, the pre-reactive complex $^3M1_{234}$, common to channels (2)−(4), and the pre-product complexes $^3M4_3$ and $^3M4_4$ disappear from the corresponding PES (see Table 4). The triplet pathway to HCO + NO presents a free energy barrier of 33.4 kcal/mol ($^3TS23_1$) and therefore is disfavored with respect to the singlet one, as already mentioned. The energy barrier for

the triplet pathway to CO + NO + H (^{3}TS12$_2$) is mainly due to the entropy contribution and is the same as that for the singlet pathway, 20.7 kcal/mol, and therefore both routes are competitive. The energy barrier for the triplet channel to HNCO + O is 11.5 kcal/mol (^{3}TS34$_3$) and the activation energy for the reverse process is 16.2 kcal/mol to compare with the reported value of 11.4 kcal/mol.[5,6] Finally, the energy barrier for the triplet pathway to NCOH + O is 29.6 kcal/mol (^{3}TS34$_4$) while that for the reverse process is 5.9 kcal/mol, in reasonable agreement with the reported value of 4.0 kcal/mol.[6] Both ^{3}TS34$_3$ and ^{3}TS34$_4$ are strongly disfavored by entropy.

At 298.15 K reactions 2 and 4 are endothermic by 9.1 and 23.7 kcal/mol, respectively, whereas reactions 1 and 3 are exothermic by 5.9 and 4.7 kcal/mol, respectively.

When the temperature is increased from 298.15 to 1000 K and further to 1500 K, all the singlet critical structures become destabilized. As a consequence, at the two higher temperatures the energy profiles proceed above the separate reactants level except for ^{1}M1$_{12}$, ^{1}M4$_{12}$, and ^{1}M5$_{12}$ which are, respectively, 18.9, 3.7, and 12.6 kcal/mol more stable than the reactants at 1000 K, and ^{1}M1$_{12}$ and ^{1}M5$_{12}$, which are slightly more stable than the reactants at 1500 K. Owing to this evolution at both 1000 and 1500 K, the pre-product complex ^{1}M3$_1$ and TS ^{1}TS3P$_2$ become transient structures on the PES, and ^{1}M3$_2$ and ^{1}TS23$_2$ become close in energy.

All the triplet critical structures become destabilized with increasing temperature except the products of reaction 1 and the final part of channel (2) (^{3}M3$_2$, ^{3}TS3P$_2$, and products (CO + NO + H)). As a consequence, the pre-product complex ^{3}M4$_1$ disappears from the PES, already at 1000 K becoming a transient structure, and at 1500 K the four triplet energy profiles proceed above the reactants except for ^{3}M3$_2$, which is 16.1 kcal/mol more stable than the reactants.

Gibbs energy barriers increase with temperature. The rate determining TSs remain the same at all temperatures except for reaction 2 where the less stable structures are ^{1}TS3P$_2$ and ^{3}TS12$_2$ at 298.15 K and ^{1}TS23$_2$ at 1000 and 1500 K, where ^{1}TS23$_2$ has practically the same energy as ^{1}M3$_2$. The most favorable route to HCO + NO remains the singlet one at higher temperatures, whereas the singlet pathway to CO + NO + H becomes the most favorable one by 6 kcal/mol at 1000 K and by 8 kcal/mol at 1500 K. At higher temperatures reaction 4 remains the most disfavored kinetically but the Gibbs energy barriers for reactions 1−3 become closer the higher the temperature so that at 1500 K reactions 1 and 2 are competitive with reaction 3. These trends would agree with the increase in the concentration of NO and the decrease in the concentration of HNCO found experimentally at higher temperatures.[6,12] It is interesting to note that reaction 2, which has been found to be a high rate and sensitive reaction by reaction-path analysis,[7] is the most favored one kinetically by the increase of temperature.

At higher temperatures the products of reactions 3 and 4 become destabilized while those of reactions 1 and 2 become more stable compared with the reactants. Thus, at 1500 K reaction 4 is endothermic by 34.7 kcal/mol, reactions 1 and 3 are exothermic by 11.2 and 0.9 kcal/mol, respectively, and reaction 2, which is endothermic at 298.15 K, becomes the most exothermic one (−24.7 kcal/mol) at 1500 K owing to the favorable entropic term.

Table 5 collects the rate constants evaluated with our theoretical Gibbs energy barriers using TST[13] at 1000 and 1500 K and the corresponding values obtained with the expressions proposed by experimentalists for this temperature range.[1,6] We see that the theoretical values are in reasonable agreement with the experimental ones. All the rate constants increase with temperature. The largest increment takes place for reaction 2 followed by reaction −3 and the smallest increment corresponds to reaction −4. These trends are reproduced by our theoretical values. The calculated rate constants are larger than those provided by the proposed expressions for reactions 1 and −4, whereas for reaction −3 the theoretically predicted value is smaller. It is interesting to note that the theoretical rate constant predicted for reaction 2 along the triplet channel agrees better than that for the singlet one with that given by the proposed expression by experimentalists, particularly the most recently reported one.[1] This could indicate that the triplet channel is dynamically more favorable than the singlet one.

TABLE 5: Rate Constants Evaluated with DFT Gibbs Energy Barriers Using TST (k_{calc}), and the Corresponding Results Obtained by Experimentalists (k_{exp})[a]

	k_{calc}		k_{exp}	
reaction	1000 K	1500 K	1000 K	1500 K
1 (singlet)	36E+09	24E+10	2.6E+09[b]	3.3E+10[b]
2 (singlet)	56E+08	18E+10		
2 (triplet)	2.8E+08	1.3E+10		
			6.1E+07[b]	8.1E+09[b]
			6.7E+08[c]	1.4E+10[c]
−3	0.32E+10	0.76E+11	1.4E+10[b]	2.2E+11[b]
−4	8.7E+11	41E+11	1.3E+11[b]	7.1E+11[b]

[a] The values are given in cm^3 mol^{-1} s^{-1}. [b] Rate constants obtained from ref 6. [c] Rate constants obtained from ref 1.

Acknowledgment. We are grateful to the FICYT (Principado de Asturias, Spain) for financial support (PB-AMB99-07C2). P.C. also thanks the FICYT for a grant (FC-99-BECA-541).

References and Notes

(1) Dean, A. M.; Bozzelly, J. W. *Gas-Phase Combustion Chemistry*; Gardiner, W. C., Jr., Ed.; Springer: New York, 2000.

(2) Miller, J. A.; Bowman, C. T. *Prog. Energy Combust.* **1989**, *15*, 287.

(3) Miller, J. A.; Bowman, C. T. *Int. J. Chem. Kinet.* **1991**, *23*, 289.

(4) Glassman, I. *Combustion*, 3rd ed.; Academic: San Diego, 1996.

(5) Warnatz, J.; Maas, U.; Dibbled, R. W. *Combustion*, 2nd ed.; Springer: Berlin, 1999.

(6) Kantak, M. V.; De Manrique, K. S.; Aglave, R. H.; Hesketh, R. P. *Combust. Flame* **1997**, *108*, 235.

(7) Schlegel, H. B. *J. Comput. Chem.* **1982**, *3*, 214.

(8) (a) Becke, A. B. *J. Chem. Phys.* **1993**, *98*, 5648. (b) Becke, A. B. *Phys. Rev. A* **1988**, *38*, 3098. (c) Lee, C.; Yang, W.; Parr, R. G. *Phys. Rev. B* **1988**, *37*, 785.

(9) Frisch, M. J.; Trucks, G. W.; Schlegel, H. B.; Scuseria, G. E.; Robb, M. A.; Cheeseman, J. R.; Zakrzewski, V. G.; Montgomery, J. A.; Stratmann, R. E., Jr.; Burant, J. C.; Dapprich, S.; Millam, J. M.; Daniels, A. D.; Kudin, K. N.; Strain, M. C.; Farkas, O.; Tomasi, J.; Barone, V.; Cossi, M.; Cammi, R.; Mennucci, B.; Pomelli, C.; Adamo, C.; Clifford, S.; Ochterski, J.; Petersson, G. A.; Ayala, P. Y.; Cui, Q.; Morokuma, K.; Malick, D. K.; Rabuck, A. D.; Raghavachari, K.; Foresman, J. B.; Cioslowski, J.; Ortiz, J. V.; Stefanov, B. B.; Liu, G.; Liashenko, A.; Piskorz, P.; Komaromi, I.; Gomperts, R.; Martin, R. L.; Fox, D. J.; Keith, T.; Al-Laham, M. A.; Peng, C. Y.; Nanayakkara, A.; Gonzalez, C.; Challacombe, M.; Gill, P. M. W.; Johnson, B.; Chen, W.; Wong, M. W.; Andres, J. L.; Gonzalez, C.; Head-Gordon, M.; Replogle, E. S.; Pople, J. A. *Gaussian 98*, Revision A.6; Gaussian, Inc.: Pittsburgh, PA, 1998.

(10) (a) Gonzalez, C.; Schlegel, H. B. *J. Chem. Phys.* **1989**, *90*, 2154. (b) Gonzalez, C.; Schlegel, H. B. *J. Phys. Chem.* **1990**, *94*, 5523.

(11) McQuarrie, D. A. *Statistical Mechanics*; Harper & Row: New York, 1986.

(12) Glarborg, P.; Miller, J. A. *Combust. Flame* **1994**, *99*, 475.

(13) Kinetic constants were computed using the conventional TST: $k = (k_B T/h) \exp(-\Delta G^{\#}/RT)$ where $\Delta G^{\#}$ is the energy barrier.